# Interfacial Effects in Polymer Nanocomposites Studied by Dielectric and Thermal Techniques

**Panagiotis Klonos, Christos Pandis, Sotiria Kripotou, Apostolos Kyritsis** and **Polycarpos Pissis**
Department of Physics, National Technical University of Athens
Heroon Polytechneiou 9
Zografou Campous, 15780, Athens, Greece

## ABSTRACT

**Effects of interfaces and interphases in polydimethylsiloxane (PDMS) matrices with *in situ* synthesized titania (20 – 40 nm, in diameter) and silica nanoparticles (~5 nm), were studied employing dielectric and thermal techniques. The presence of the well dispersed inorganic particles and the hydrogen polymer - filler bonding result in a double effect on polymer mobility: suppression of crystallization and immobilization in a layer of a few nm around the particles. The effects were stronger in the case of titania nanoparticles, in consistency with stronger hydrogen bonding interactions, comparing to silica. Various contributions to the glass transition were recorded by both thermal and dielectric techniques, corresponding to bulk and modified polymer dynamics. The modified mobility originates from the restriction of polymer chains within the PDMS crystals and in an interafacial rigid amorphous PDMS layer around the nanoparticles. The thickness of the interfacial layer was estimated to 3-5 nm for titania and ~2 nm for silica. The mobile amorphous phase fraction giving rise to the glass transition was found to be nearly constant in the nanocomposites. The results were confirmed by employing various thermal (crystallization) treatments of the samples.**

Index Terms — **Polydimethylsiloxane, nanoparticles, silica, titania, polymer crystallization, glass transition, segmental dynamics, interfacial interactions, dielectric spectroscopy.**

## 1 INTRODUCTION

**NANOCOMPOSITE** materials, in particular polymer nanocomposites, may provide solution to modern industrial, biophysical and even domestic needs [1-2]. The advantage of such nanomaterials, comparing to traditional composites, is the significant improvement of good properties of the polymer matrix with the use of relatively low nanofiller loadings [3]. The origins of the high level of improvement is still an open debate in the basic research community, but the most prevailing opinion is that the high volume to surface ratio of nanoparticles leads to significant changes in molecular mobility and distribution of polymer chains close (some or tens of nanometers) to the surface of the particles. Seeking for evidences of the modified molecular mobility has been attempted by various research groups using various techniques [4-8]. The results show that the presence of nanofillers (e.g. silica, clays, nanotubes) and their interaction with the matrix may increase or decrease molecular mobility [1, 9-10] and crystallization ability [11-12]. The presence of polymer crystals can also modify the bulk polymer dynamics, offering similar effects as the nanoparticles [13-18]. Thus, filler addition may affect directly or indirectly molecular structure and dynamics of the polymer matrix. For semicrystalline polymer matrices filled with inorganic nanoparticles, the so called '3 layer model' [6] can describe well the experimental results. According to that model, one can separate the energy contribution of the crystalline phase (CR), the mobile amorphous phase (MAF) and the rigid amorphous phase (RAF), mainly in a differential scanning calorimetry study.

In the present study thermal (differential scanning calorimetry - DSC) and dielectric techniques (dielectric relaxation spectroscopy – DRS and thermally stimulated depolarization currents - TSDC) are combined to study interfacial effects in polymer nanocomposites. Following previous work [12, 18-19], we focus on materials based on a rubbery matrix (polydimethylsiloxane, PDMS) filled with *in situ* synthesized inorganic nanoparticles (titania and silica, via sol-gel method) [20]. Novel aspects of this study are the thermal treatment of the materials prior to thermal and dielectric measurements to appropriately tune the degree of crystallinity and check various hypotheses, the direct comparison of DSC-TSDC data recorded in the region of the glass transition, and the analysis of DSC thermograms in terms of various contributions to the glass transition.

*Manuscript received on 15 November 2011, in final form 2 May 2012.*

# 2 EXPERIMENTAL

## 2.1 MATERIALS

PDMS networks filled with silica and titania nanoparticles and, for comparison, unfilled PDMS network were prepared. Unfilled PDMS network was synthesized from hydroxyl-terminated PDMS (Gelest, Mw=18000) by end-linking reactions with tetraethoxysilane (TEOS) as cross-linking agent. The unfilled PDMS network was swollen in TEOS and titanium (IV) n-butoxide (TBO) for silica and titania nanocomposites preparation, respectively. The samples were hydrolyzed during 48 h and finally vacuum-dried at 80 °C for five to seven days to constant weight. The amount of filler was calculated from the weight before and after the generation of the filler and was varied between 6 and 36 wt% in silica nanocomposites and between 5 and 18 wt% in titania nanocomposites. Films of ~1 mm in thickness were prepared [20]. Transmission electron microscopy (TEM) and small-angle neutron scattering (SANS) measurements [20] showed a very good dispersion of silica nanoparticles with a mean diameter of about 5 nm and of titania nanoparticles with diameters between 20 and 40 nm. For high filler contents an interpenetrated polymer-oxide structure was obtained. Mechanical and swelling measurements showed higher reinforcement of PDMS in the case of silica, due to the higher surface to volume ratio [20].

## 2.2 TECHNIQUES

Morphology was examined by field emission Scanning Electron Microscopy. FEI NovaSEM 230 operating in high vacuum mode, using either Everhard-Thornley (ETD) or Through Lens (TLD) detector was used. Prior to the measurement a golden thin layer was developed by sputtering.

Differential scanning calorimetry (DSC) was employed to investigate thermal transitions. Measurements were carried out in helium atmosphere in the temperature range from -170 to 40 $^{o}$C at a constant cooling and heating rate of 10 $^{o}$C/min. Samples of ~8 mg were enclosed in standard Tzero aluminium pans. In order to investigate the effects of crystallinity on the glass transition, measurements were carried out also after annealing of the samples at a temperature between the onset and the peak temperature of crystallization, as defined by typical DSC measurements, for 30 min (enhanced crystallinity), and after quenching (suppressed crystallinity). A cooling rate of 40 $^{o}$C/min was achieved in the crystallization region (-70 to -110 $^{o}$C) [21]. For DSC measurements the TA Q200 instrument was used.

Thermally stimulated depolarization currents (TSDC) is a special dielectric technique in the temperature domain. TSDC is characterized by high sensitivity and high resolving power, the latter arising from its low equivalent frequency ($10^{-4}$–$10^{-2}$ Hz) [22]. The sample was inserted between the plates of a capacitor. The thickness of the samples was ~1 mm while their diameter was varying between 12 and 20 mm. The capacitor was placed in a Novocontrol TSDC sample cell and polarized by the application of an electric field $E_p$ equal to ~100 V/mm at a polarization temperature $T_p$ of 20 $^{o}$C for a polarization time $t_p$ of 5 min. With the electric field still applied, the sample was cooled down to -150 $^{o}$C (cooling rate 10 $^{o}$C/min, under nitrogen flow), sufficiently low to prevent depolarization by thermal energy, then short-circuited and reheated up to 50 $^{o}$C at a constant rate $b$ of 3 $^{o}$C/min. The discharge current generated during heating was recorded as a function of temperature [8, 12, 17, 22]. In order to facilitate direct comparison with the crystallization annealing DSC measurements, same thermal treatment of the samples was performed for TSDC measurements. Temperature control was achieved by means of a Novocontrol Quatro cryosystem while the current was recorded by the Keithley 617 electrometer.

For dielectric relaxation spectroscopy (DRS) measurements [23] the sample (same as that used for TSDC measurements) was placed between the plates of a capacitor and an alternate voltage was applied in a Novocontrol sample cell. The complex dielectric permittivity, $\varepsilon^*=\varepsilon'-i\varepsilon''$, was recorded isothermally as a function of frequency in the range from $10^{-1}$ to $10^{6}$ Hz. The measurements were carried out in the temperature range from -150 to 20 $^{o}$C in steps of 2.5, 5 and 10 $^{o}$C depending on the process followed [8, 10-12, 16-17, 22]. Measurements were carried out after linear cooling and after annealing of the samples at a temperature between the onset and the peak temperature of crystallization, as defined by DSC measurements, for 30 min. DRS measurements were carried out by means of a Novocontrol Alpha analyzer while temperature was controlled to better than 0.5 $^{o}$C by a Novocontrol Quatro cryosystem.

# 3 RESULTS AND DISCUSSION

## 3.1 SCANNING ELECTRON MICROSCOPY - SEM

Representative SEM pictures for PDMS with low and higher titania loadings are presented in Figure 1. Pictures were taken at room temperature, so we expect to monitor the dispersion of the nanoparticles in the amorphous (melted) PDMS matrix. Previous study of these systems showed that PDMS gets crystallized at temperatures between -70 and -100 $^{o}$C and melts at about -40 $^{o}$C [12, 18]. Indeed in Figure 1a and 1b one can identify the well dispersed nanoparticles. In the higher loading, larger particle domains (100 - 200 nm in diameter) can be also identified. TEM results on the same systems, published elsewhere [20], showed that the diameter of the nanoparticles is around 20 – 40 nm for titania and 5 nm for silica. Additionally, the formation of silica and titania structures (networks) was reported for high loadings [20]. SEM results in Figure 1 along with the respective images for PDMS/silica (not shown here) come in agreement and supplement the TEM measurements.

## 3.2 DIFFERENTIAL SCANNING CALORIMETRY – DSC

Representative DSC cooling scans, at 10 $^{o}$C/min, of unfilled PDMS and its titania and silica nanocomposites are shown in Figure 2. Single crystallization peaks were recorded at temperatures between -100 and -75 $^{o}$C. In general, the addition of filler leaded to lower crystallization temperatures, $T_C$, and lower crystallization enthalpies, $\Delta H_C$ [12]. These

results suggest that the nanoparticles do not act as crystallization nuclei and the polymer crystals grow away from the inorganic surfaces. According to polymer physics [24], more crystals and larger in size should be present in neat PDMS than in the nanocomposites, as $T_C$ and $\Delta H_C$ get gradually lower with increasing filler content [12]. In the case of faster cooling (~40 °C/min, in the crystallization temperature region) all the crystallization peaks (not shown here) were energetically suppressed (~10 %) and shifted to lower temperatures (by 5-20 °C). The suppression of crystallization ability was stronger in the case of titania nanocomposites. On the other hand, in the case of crystallization annealing the degree of crystallinity, $X_C$, was increased by ~10 %. The glass transition was recorded in the temperature range between -130 and -115 °C, as we can follow in Figures 2 and 3, without any significant variation in the temperature position. The interesting point is the temperature development of the glass transition step and its changes with increasing filler content.

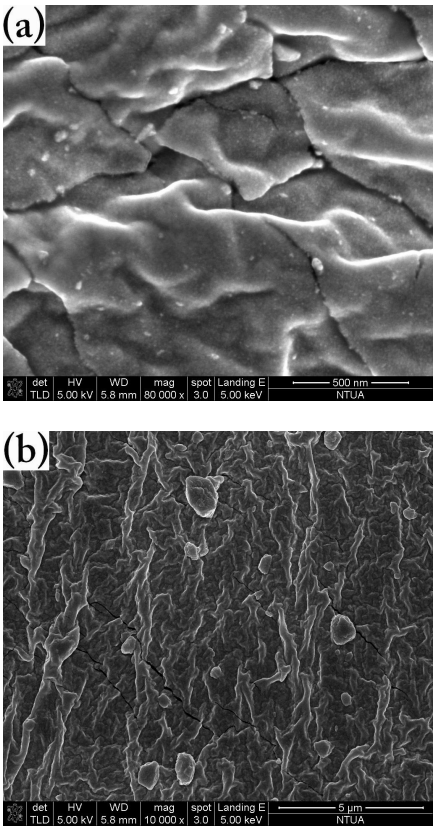


**Figure 1.** SEM images for (a) PDMS + 4 wt% $TiO_2$ and (b) PDMS + 15 wt% $TiO_2$.

In Figures 3a and 3b one can easily notice that the glass transition shape, after standard cooling, is single and smoothed for the unfilled PDMS (Figure 3a) and seems to be double structured in the case of nanocomposites (Figure 3b, for PDMS + 18 wt% titania, representing the nanocomposites). with 31 wt% silica and 11.5 wt% titania and higher. As filler content increases the height of the first contribution (low-temperature side, trend 2 in Figure 3b) is increased, in terms of heat capacity change $\Delta C_p$, while at the same time the secondary contribution at the high-temperature side (trend 3 in Figure 3b) gets more clear [12]. Similar results were reported before in PDMS [18], PVP [25] and PVA [26] nanocomposites. The secondary contribution (trend 3) seems to dominate the response of the samples in the case of heating after crystallization annealing. On the other hand, fast cooling leads to suppression of crystallization (quenching [21]), resulting in an increase of the first contribution (sharp step, trend 2). The first and secondary contribution seem to be related to unaffected (bulk) amorphous mobility and to interphase (amorphous - crystalline polymer) interactions, respectively. This point will be further discussed later in this section and also in combination with TSDC and DRS results.

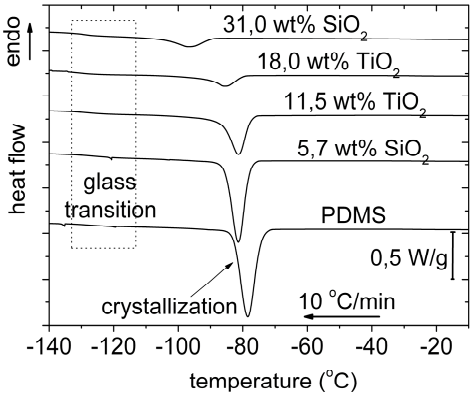


**Figure 2.** DSC thermograms for unfilled PDMS, PDMS/silica and PDMS/titania nanocomposites during cooling at 10 °C/min.

At temperatures around -90 °C during cooling (Figure 3) an exothermic peak is observed in the nanocomposites of high loadings after standard cooling, and in all samples [12] after fast cooling. This event corresponds to cold crystallization and originates from uncompleted crystallization during cooling [19, 24]. The event is logically absent in the case of crystallization annealing. At higher temperatures (between -70 and -40 °C) a complex endothermic peak is recorded for all the samples. The lower temperature contribution, named *peak 1* in Figure 3, and the main one, at higher temperatures, named *peak 2*, were both enhanced after crystallization annealing. Peak 1 was almost eliminated after faster cooling. Judging from the lower melting temperature values of peak 1 and the SEM microghaphs of PDMS crystalline morphology by Sundararajan [27], we get strong indications that peak 1 corresponds to the melting of secondary small (~ 1 μm) and low quality spherulites of PDMS, which grow in the amorphous islands between the primary large (~ 100 μm) spherulites.

Coming back to the glass transition, we focus on a quantitave estimation of the various polymer fractions (Figures 4 and 5) on the basis of the change in the heat capacity at the glass transition, $\Delta C_p$. The recorded $\Delta C_p$ was normalized [12, 18] to the uncrystallized polymer fraction

for all the samples, while passing from the glassy to the rubbery state, during heating. The respective values of $\Delta C_{p,norm}$ were found to decrease on the addition of filler. That was a sign of uncrystallized polymer immobilized (rigid amorphous) or confined in the organic-inorganic system, which does not participate in the glass transition. Two types of rigid amorphous polymer fractions (RAF) are reported in the literature. The first is affiliated to the strong interactions of the polymer chains with the nanoparticles, $RAF_{filler}$, the effect of which extends from some to tens nanometers [5-6, 8, 15]. The second one is affiliated to the organic chains which are semi bound within the polymer crystals, $RAF_{cryst}$, the 'immobilization' of which was studied by various techniques [13-14, 16]. In Figure 4 a scheme of the estimated distribution of filler, crystalline polymer (CR), mobile amorphous (MAF) and rigid amorphous (RAF) polymer in the nanomaterials is presented.

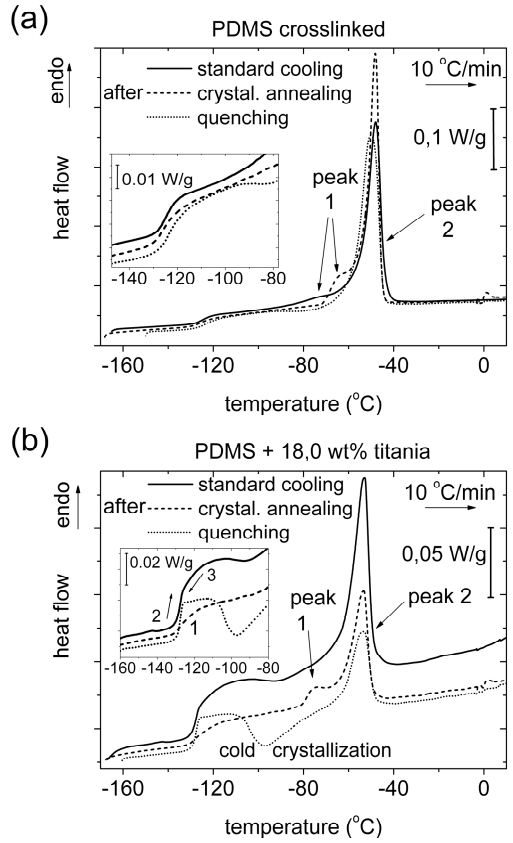


**Figure 3.** DSC thermograms for: (a) unfilled PDMS and (b) PDMS + 18 wt% $TiO_2$ during heating at 10 °C/min, after different cooling (crystallization) treatments.

Figure 5 summarizes the composition map of PDMS/titania and PDMS/silica in the temperature region of glass transition. In the case of PDMS/silica, the composition diagrams are given for the three crystallization treatments followed. For the same filler loadings, similar values are obtained for RAF for PDMS/titania and PDMS/silica nanocomposites. In the case of crystallization annealing or fast cooling (quenching), RAF was increased or reduced, respectively. The additional or residual RAF amount, should correspond to $RAF_{cryst}$. A quite interesting observation in all cases is that the mobile amorphous polymer fraction (MAF, i.e. the fraction which participates in the glass transition) is almost constant in the same series of samples and same crystallization treatment. This fact suggests a thermodynamic balance between the multiphase mobility in our systems [28]. At this point, we should mention that the crystalline PDMS fraction (CR) was calculated via the crystallization enthalpy for standard and fast cooling and from the respective melting enthalpy for the annealing treatment. Additionally, the equations used for our calculations [12] are not suitable for separate calculations of $RAF_{cryst}$ and $RAF_{filler}$. Such calculations may be done firmly after Temperature Modulated DSC measurements [13, 21] and the application of bibliographic data (i.e. ATHAS databank) [6, 13]. Thus, we should keep in mind for the following that in Figure 5 the CR fraction of the unfilled PDMS should also include the respective $RAF_{cryst}$.

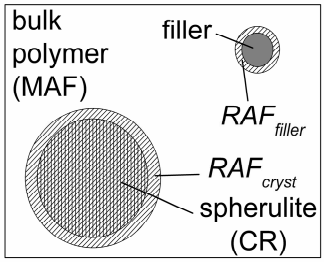


**Figure 4.** A simplified model of the estimated distribution of the different polymer phases (crystalline, mobile amorphous and rigid amorphous) and filler.

### 3.3 THERMALLY STIMULATED DEPOLARIZATION CURRENTS – TSDC

TSDC thermograms are presented in Figure 6, for the unfilled crosslinked PDMS in Figure 6a and for the higher loadings of titania in Figure 6b, under the normal and annealing crystallization treatments. In Figure 6a we added measurements of linear PDMS ($M_w$~8000) to be commented on later. The depolarization signals were normalized with the applied electric field, so that results for different samples can be compared to each other not only with respect to the temperature position of the peak (time scale of the corresponding relaxation) but also with respect to the magnitude of the peak (dielectric strength of the corresponding relaxation).

In the temperature range between -140 and -100 °C the recorded peaks correspond to the dielectric response of the glass transition, as the equivalent frequencies of DSC and TSDC are quite close [12]. At higher temperatures between -95 and -80 °C we recorded negative peaks, most possibly related to the cold crystallization events, as they were observed only in the cases of sample where we recorded cold crystallization by DSC. In the temperature region from -65 to -40 °C the disordered noise-type signals correspond to the massive disengagement of electrical charges, while the samples approach their melting points and the polymer

crystals get destroyed. These results were confirmed by TSDC measurements (not shown here) without the application of electric field.

In Figure 6a the glass transition of our crosslinked unfilled PDMS ($X_C$~0.90) is expressed exclusively by the $\alpha_C$ peak, at ~ -122 $^oC$. In previous work [12, 18] this peak was correlated to the relaxation mechanism of amorphous polymer confined between condensed crystal regions [16]. It is interesting to note that the response of linear PDMS ($X_C$~0.60) was dominated by the sharp $\alpha$ relaxation, which characterizes the bulk behaviour of the polymer [12]. In the case of nanocomposites, three peaks ($\alpha$, $\alpha_c$ and $\alpha'$ relaxations) contribute to the complex segmental dynamics trace in a systematic manner, in order of increasing temperature. The $\alpha'$ relaxation (between -95 and -110 $^oC$) is present only in the nanocomposites and its magnitude increases with filler content. There are strong indications that $\alpha'$ relaxation is the segmental mobility mechanism of the polymer chains which are bound on the surfaces of the nanoparticles [12, 17-18]. Observed at about -123 $^oC$, $\alpha_c$ is slower and stronger than $\alpha'$ and its position is not affected by the addition of the nanoparticles. The strength of this relaxation decreases with decreasing degree of crystallinity. Simultaneously with the depression of $\alpha_c$ the upcoming of $\alpha$ relaxation is observed at -130 to -128 $^oC$. For the high filler contents (both for silica and titania) $\alpha$ relaxation dominates (Figure 6b) while the degree of crystallinity is minimized. After the annealing of crystallization, the response in these samples, where $X_C$ increased by 20 – 30 %, is dominated by the $\alpha_C$ relaxation. At the same time, the inverted peaks at higher temperatures (cold crystallization) were logically vanished and the melting TSDC events were enhanced.

The most interesting result comes from the direct comparison between DSC and TSDC thermograms, presented in common diagrams in Figure 7. The thermograms for standard and annealed crystallization are shown for the unfilled linear PDMS (Figure 7a) and PDMS + 31 wt% silica nanocomposite (Figure 7b). The sharp $\alpha$ relaxation has almost the same temperature position and temperature evolution with the low temperature contribution to the calorimetric glass transition (trend 2 in Figure 3). The $\alpha_C$ relaxation shows similar behaviour with the higher temperature contribution to glass transition (trend 3 in Figure 3). The question arises as to whether we have recorded at the same sample the glass transition of bulk and bound behaviour. Cebe et al [13] recorded calorimetrically the relaxation of $RAF_{cryst}$ of isotactic polystyrene (iPS) as an endothermic glass transition step at temperatures close to the melting point. Additionally, trend 3 in Figure 3 or the indicated $T_g'$ may also match with the $\alpha'$ relaxation (Figure 7b) of the PDMS interfacial layer. According to Schick and coworkers [5], this part of the polymer will remain rigid until the temperature of decomposition of the polymer, or, in general, the reason for keeping it rigid (i.e. interfacial interactions), so it is not possible to record a respective glass transition.

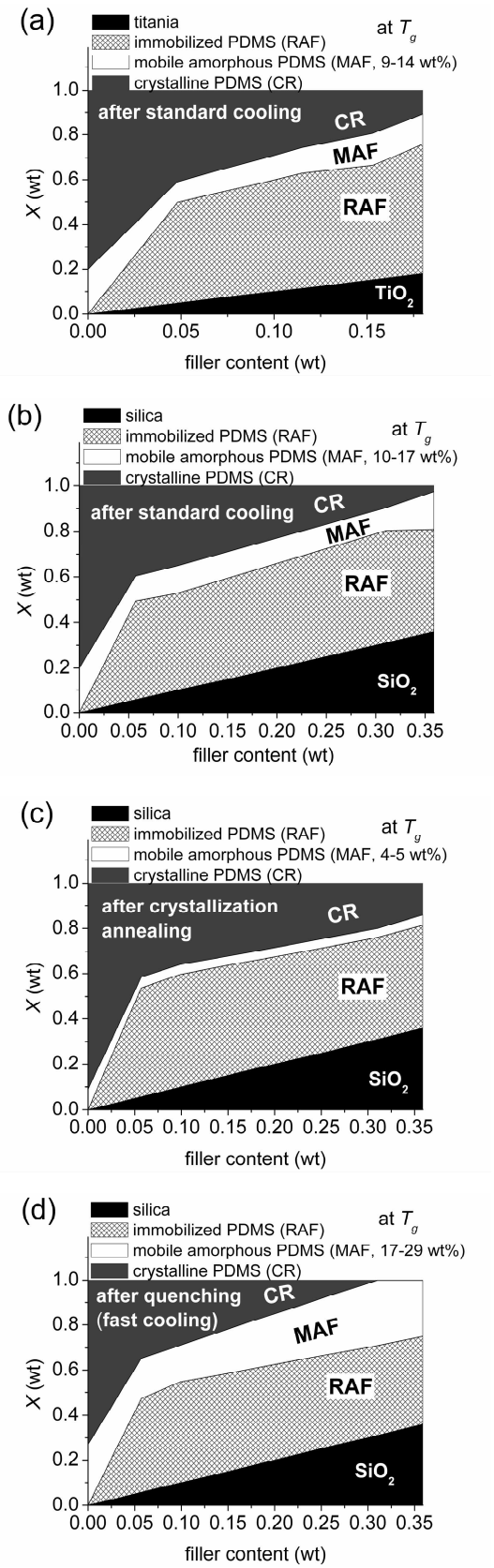


**Figure 5.** Composition (wt) diagrams for PDMS and its nanocomposites in the region of the glass transition. Referring to filler type (a) corresponds to PDMS/titania and (b) to PDMS/silica. Referring to different crystallization treatments of PDMS/silica, (b) corresponds to continuous linear cooling, (c) to crystallization annealing and (d) to fast cooling (quenching).

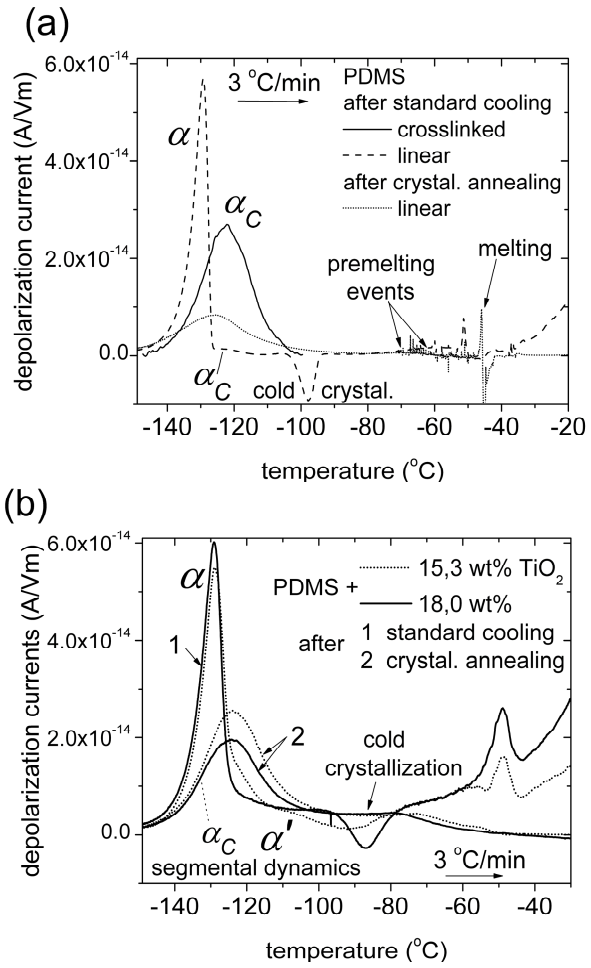


**Figure 6.** Comparative TSDC thermograms for (a) unfilled PDMS (included is the respective measurement for linear PDMS with similar molecular weight) and (b) PDMS/titania nanocomposites, after standard cooling (solid lines) and crystallization annealing (dotted lines).

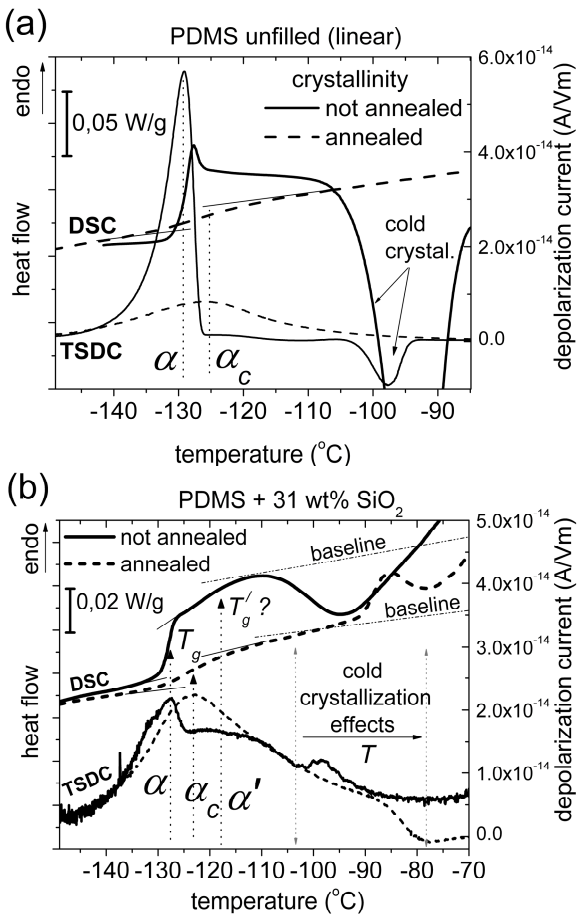


**Figure 7.** Comparative TSDC and DSC thermograms in the temperature region of glass transition and crystallization for (a) linear PDMS and (b) PDMS + 31 wt% silica nanocomposite, after standard cooling (solid lines) and crystallization annealing (dotted lines).

We should also keep in mind that the presence of the cold crystallization peak, quite close to the glass transition in the DSC thermograms, renders evaluation rather difficult. Further measurements, in particular by employing TMDSC measurements [21], could illuminate these points. The dielectric strength, $\Delta\varepsilon$, [23] of the relaxations recorded by TSDC was calculated and the respective interfacial polymer fraction $X_{int}$ was estimated, as in previous work [12]. This point will be discussed in the DRS section, as similar calculations were made there.

### 3.4 DIELECTRIC RELAXATION SPECTROSCOPY - DRS

Recorded DRS results are similar to those reported in previous work [12] and will not be shown here. Instead, we focus on the analysis of DRS data, in particular with respect to the fraction of interfacial polymer (Figure 8) and the time scale of the various relaxations (Figure 9), focusing mainly on the effects of different polymer-filler interactions and the interfacial amorphous – crystallized polymer interactions.

In Figure 8 we present a comparison of the interfacial PDMS fraction, $X_{int}$, for different filler loadings. The modified mobility of the interfacial polymer is recorded through the $\alpha'$ dielectric relaxation mechanism [12, 18]. The calculations were done by dividing the dielectric strength of $\alpha'$ relaxation, ($\Delta\varepsilon_{\alpha'}$), with the sum of the dielectric relaxation strengths of $\alpha$, $\alpha_C$ and $\alpha'$ relaxations, ($\Delta\varepsilon_{\alpha'}+\Delta\varepsilon_{a+ac}$), and normalizing with the uncrystallized polymer fraction, ($1-X_c$), as calculated by DSC [12], for the standard and annealing crystallization treatments. The results show that in the case of PDMS/silica the interfacial polymer fraction increases up to 0.55 for the highest filler contents (Figure 8), while in the case of PDMS/titania $X_{int}$ is significantly lower and increases up to 0.14 for the highest loading (Figure 8). The higher values of interafacial fraction for PDMS/silica are possibly affiliated to the higher surface to volume ratio and the weaker polymer-filler bonds, compared to PDMS/titania. This second statement is confirmed by the different trace of $\alpha'$ relaxation (discussed later in Figure 9) for silica and titania nanocomposites. As reported before, it is very interesting, from the methodological point of view, that the results for $X_{int}$ agree very well with those calculated from the TSDC thermograms. Assuming spherical nanoparticles, we estimated that the thickness of the PDMS interfacial layer, $d_{int}$ [18], is 3-

5 nm for PDMS/titania and ~2 nm for PDMS/silica nanocomposites.

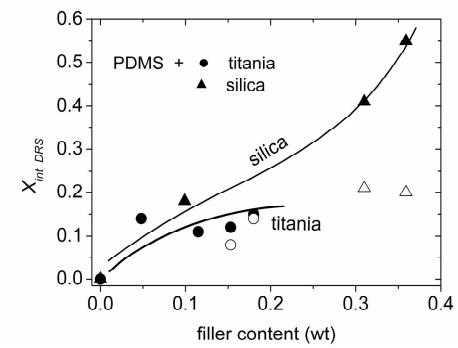


**Figure 8.** Fraction of interfacial PDMS vs filler content, obtained for PDMS/silica and PDMS/titania nanocomposites from DRS measurements after standard cooling at 10 °C/min (solid symbols) and crystallization annealing (open symbols). Lines were added as guides for the eyes.

Figure 9 summarizes DRS results on the time scale of the three segmental relaxations mentioned above in terms of the activation diagram for representative samples. A main observation in Figure 9 is that $\alpha$ and $\alpha_c$ have very similar frequency-temperature traces, both of the Vogel-Tammann-Fulcher (VTF) type [29], characteristic for segmental dynamics. The time scale of these relaxations is practically not affected by the addition of nanoparticles. Observed at lower frequencies/higher temperatures, $\alpha'$ is strongly separated from $\alpha$ and $\alpha_c$. $\alpha'$ relaxation is also described by VTF but with lower activation energies and fragility, as compared to $\alpha$ and $\alpha_c$. The latter is reasonable in terms of lower cooperativity length [6, 18].The time scale of $\alpha'$ relaxation is almost identical for all the PDMS-silica nanocomposites (open symbols in Figure 9). $\alpha'$ relaxation for PDMS/titania nanocomposites is shifted to higher temperatures/lower frequencies, as compared to PDMS/silica, (solid symbols in Figure 9), showing again similar time scale for all the PDMS/titania samples. One could suggest that the shift on the traces of this relaxation is indicative of the difference on the polymer-filler interaction strength, which is higher in the case of PDMS/titania.

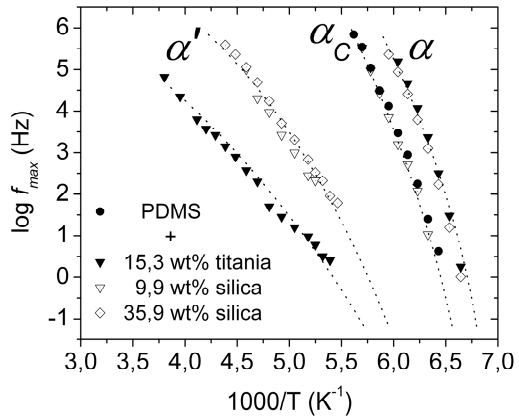


**Figure 9.** Activation diagram (Arrhenius plots) of the segmental mobility relaxations ($\alpha$, $\alpha_C$ and $\alpha'$) for PDMS, PDMS + 15,3 wt% titania, PDMS + 9,9 wt% silica and PDMS + 35,9 wt% silica nanocomposites, as recorded from the isothermal DRS measurements. Lines were added as guides for the eyes.

# 5 CONCLUSION

DSC measurements on various PDMS nanocomposites using different thermal treatments showed that the good dispersion and strong polymer/filler interactions restrict crystallization and segmental mobility of the polymer. A systematic reduction of the heat capacity step of glass transition with the addition of filler was attributed to the so called 'immobilized polymer-filler interfacial layer' (RAF). This layer was estimated to 80 wt% of the uncrystallized polymer fraction. Different crystallization treatments of the samples, revealed a balance between the crystalline and rigid amorphous polymer, represented by an almost constant mobile amorphous PDMS fraction (MAF) in the nanocomposites. On the other hand, the dielectric techniques (DRS, TSDC) were able to record the reduced mobility of this layer, and revealed discrete contributions to segmental dynamics of the polymer and the corresponding glass transition, related to specific interactions and topology. Further measurements, including thermal sampling TSDC [18], are expected to shed more light on this point. The thickness of the interfacial layer $d_{int}$ was calculated to be 3-5 nm for PDMS/titania and ~2 nm for PDMS/silica nanocomposites form the DRS results. Analysis and further work in progress, including measurements on fumed silica and titania with sorbed PDMS, may lead to a more quantitative description of the various contributions.

# ACKNOWLEDGMENT

The authors would like to thank Professor Liliane Bokobza, E.S.P.C.I., Paris, France, for providing the materials.

This research has been co-financed by the European Union (European Social Fund – ESF) and Greek national funds through the Operational Program 'Education and Lifelong Learning' of the National Strategic Reference Framework (NSRF) – Research Funding Program: Heracleitus II. Investing in knowledge society through the European Social Fund.

# REFERENCES

[1] D. R. Paul, and L. M. Robenson, "Polymer nanotechnology: nanocomposites", Polymer, Vol. 49, pp. 3187-3204, 2008.

[2] J. Jancar, J. F. Douglas, F. W. Starr, S. K. Kumar, P. Cassagnau, A. J. Lesser, S. S. Sternstein, and M. J. Buehler, "Current issues in research on structure-property relationships in polymer nanocomposites", Polymer, Vol. 51, pp. 3321-3342, 2010.

[3] L. Bokobza, and J. P. Chauvin, "Reinforcement of natural rubber: use of in situ generated silicas and nanofibres of sepiolite", Polymer, Vol. 46, pp. 4144-4151, 2005.

[4] S. Napolitano, and M. Wubbenhorst, "The lifetime of deviations from bulk behaviour in polymers confined at the nanoscale", Nat. Commun., Vol. 2, No. 260, 2010.

[5] A. Sargsyan, A. Tonoyan, S. Davtyan, and S. Schick, "The amount of immobilized polymer in PMMA SiO2 nanocomposites determined from calorimetric data", Eur. Polym. J., Vol. 43, pp. 3113-3127, 2007.

[6] A. Wurm, M. Ismail, B. Kretzschmar, D. Pospiech, and C. Schick, "Retarded crystallization in polyamide/layered silicates nanocomposites caused by an immobilized interphase", Macromolecules, Vol. 43, pp. 1480-1487, 2010.

[7] K. Parker, R. T. Schneider, R. W. Siegel, R. Ozisik, J. C. Cabanelas, B. Serrano, C. Antonelli, and J. Baselga, "Molecular probe technique for determining local thermal transitions: the glass transition at silica/PMMA nanocomposite interfaces", Polymer, Vol. 51, pp. 4891-4898, 2010.

[8] J. F. Capsal, E. Dantras, J. Dandurand, and C. Lacabanne, "Molecular mobility in piezoelectric hybrid nanocomposites with 0-3 connectivity: particles size influence", J. Non-Cryst. Solids, Vol. 357, pp. 3410-3415, 2011.
[9] S. E. Harton, S. K. kumar, H. Yang, T. Koga, K. Hicks, H. Lee, J. Mijovic, M. Liu, R. S. Vallery, and D. W. Gidley, "Immobilized polymer layers on spherical nanoparticles", Macromolecules, Vol. 43, pp. 3415-3421, 2010.
[10] V. M. Boucher, D. Cangialosi, A. Alegria, J. Colmenero, J. Gonzalez-Irun, and L. M. Liz-Marzan, "Physical aging in PMMA/silica nanocomposites: enthalpy and dielectric relaxation", J. Non-Cryst. Solids, Vol. 357, pp. 605-607, 2011.
[11] E. Logakis, C. Pandis, V. Peoglos, P. Pissis, C. Stergiou, J. Pionteck, P. Poetchke, M. Micusik, and M. Omastova, "Structure-property relationships in polyamide 6/multi-walled carbon nanotubes nanocomposites", J. Polym. Sci. B Polym. Phys., Vol. 47, pp. 764-774, 2009.
[12] P. Klonos, A. Panagopoulou, L. Bokobza, A. Kyritsis, V. Peoglos, and P. Pissis, "Comparative studies on effects of silica and titania nanoparticles on crystallization and complex segmental dynamics in poly(dimethylsiloxane)", Polymer, Vol. 51, pp. 5490-5499, 2010.
[13] H. Xu, and P. Cebe, "Heat capacity study of isotactic polystyrene: dual reversible crystal melting and relaxation of rigid amorphous fraction", Macromolecules, Vol. 37, pp. 2797-2806, 2004.
[14] J. Lin, S. Shenogin, and S. Nazarenko, "Oxygen solubility ans specific volume of rigid amorphous fraction in semicrystalline poly(ethylene terephthalate)", Polymer, Vol. 43, pp. 4733-4743, 2002.
[15] Y. Miwa, A. R. Drews, and S. Schick, "Detection of the direct effect of clay on polymer dynamics: The case of spin-labeled poly(memyl acrylate)/clay nanocomposites studied by ESR, XRD, and DSC", Macromolecules, Vol. 39, pp. 3304-3311, 2006.
[16] P. Huo, and P. Cebe, "Temperature-dependent relaxation of the crystal-amorphous interphase in poly(ether ether ketone)", Macromolecules, Vol. 25, pp. 902-909, 1992.
[17] D. Fradiadakis, L. Bokobza, and P. Pissis, "Dynamics near the filler surface in natural rubber-silica nanocomposites", Polymer, Vol. 52, pp. 3175-3182, 2011.
[18] D. Fragiadakis, P. Pissis, and L. Bokobza, "Glass transition and molecular dynamics in poly(dimethylsiloxane)/silica nanocomposites", Polymer, Vol. 46, pp. 6001-6008, 2005.
[19] M. I. Aranguren, "Crystallization of polydimethylsiloxane: effect of silica filler and curing", Polymer, Vol. 39, pp. 4897-4903, 1998.
[20] L. bokobza, and A. L. Diop, "Reinforcement of poly(dimethylsiloxane) by sol-gel in situ generated silica and titania particles", Express Polym. Lett., Vol. 4, pp. 355-363, 2010.
[21] M. Sorai (Ed.), *Comprehensive handbook of calorimetry and thermal analysis*, Wiley: West Sussex, 2004.
[22] A. Kyritsis, M. Siakantari, A. Vassilikou-Dova, P. Pissis, and P. Varotsos, "Dielectric and electrical properties of polycrystalline rocks at various hydration levels", IEEE Trans. Dielectr. Electr. Insul., Vol. 35, pp. 493-497, 2000.
[23] F. Kremer, and A. Schoenhals (Eds.), *Broadband dielectric spectroscopy*, Springer, Berlin, 2002.
[24] U. W. Gedde, *Polymer physics*, Chapman & Hall, London, UK, 1995.
[25] V. A. Bershtein, V. M. Gun'ko, L. M. Egorova, N. V. Guzenko, V. A. Ryzhov, and V. I. Zarko, "Well-defined oxide core-polymer shell nanoparticles: interfacial interactions, peculiar dynamics, and transitions in polymer nanolayers", Langmuir, Vol. 26, pp. 10968-10979, 2010.
[26] L. Chen, K. Zheng, K. Hu, R. Wang, C. Liu, Y. Li, and P. Cui, "Double glass transitions and interfacial immobilized layer in in-situ-synthesized poly(vinyl alcohol)/silica nanocomposites", Macromolecules, Vol. 43, pp. 1076-1082, 2010.
[27] P. R. Sundararajan, "Crystalline morphology of poly(dimethylsiloxane)", Polymer, Vol. 43, pp. 1691-1693, 2002.
[28] J. Khan, S. E. Harton, P. Akcora, B. C. Benicewicz, and S. K. Kumar, "Polymer crystallization in nanocomposites: special reorganization of nanoparticles", Macromolecules, Vol. 42, pp. 5741-5744, 2009.
[29] E. Donth (Ed.), *The glass transition: relaxation dynamics in liquids and disorderedmaterials*, Springer series in materials science, Vol. 48, Springer, Berlin, 2001.

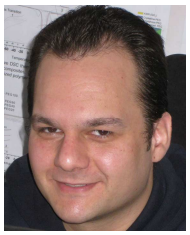

**Panagiotis Klonos** was born in Athens, Greece in 1982. He received his Applications Physicist Diploma in 2007 and the M.Sc. degree in microsystems and nanodevices in 2009, both from the National Technical University of Athens-NTUA. Currently, he is a Ph.D. degree student in the Physics Department of NTUA. He performs Thermal, Dielectric and Water Sorption measurements on various amorphous and semicrystalline polymer nanocomposites materials.

**Christos Pandis** was born in Athens, Greece in 1978. He graduated from the University of Athens in 2003 with a Diploma in physics. He obtained the M.Sc. degree in microsystems and nanodevices in 2005 and the PhD. degree on the "Development and study of polymeric materials for use in chemical sensors" in 2010, both at the National Techical University. The work of Dr. Pandis deals mainly with the structure-properties relationships in polymer nanocomposites (pncs) (thermal, mechanical, electrical/dielectric properties), gas sensing properties of polymers and pncs, structural health monitoring of advanced pncs andHydration properties of hydrogels and hybrid materials.

**Sotiria Kripotou** was born in Sparta, Greece in 1976. She received the Diploma in physics in 1999 at the University of Crete, the M.Sc. degree in physics in 2001 and the Ph.D. degree in physics in 2005, both at the National Technical University of Athens-NTUA. She has published 17 journal papers, 6 papers in conference proceedings and 2 book chapters. Her research activities include structure-property relationships studies in polymers with complex architecture (e.g. hybrid polymer networks, hyperbranched polymers, liquid crystalline polymers, diblock copolymers) and in polymer nanocomposites.

**Apostolos Kyritsis** was born in Berlin, Germany in 1966. He received the Diploma in physics in 1988 and the Ph.D. degree in materials science - physics in 1995 both by the University of Athens, Greece. He has published more than 60 scientific papers, more than 20 papers in conference proceedings and 3 book chapters. His scientific interests include dielectric, calorimetric and vapor sorption studies in ionic crystals, ceramics, polymers and complex polymeric systems and structure-property relationships in polymers, biopolymers, nanocomposites. Dr Kyritsis has been involved in national and international standardisation activities working at the Greek National Standardization Body (ELOT) between 2000 and 2005 and is also strongly interested in the metrology aspects of experimental measurements.

**Polycarpos Pissis** was born in Cyprus in 1947. He received the Diploma in physics in 1973 and the Ph.D. degree in physics in 1977 both from the University of Goettingen, Germany. He is Professor at the Physics Department, National Technical University of Athens - NTUA, Greece. He teaches several subjects, both at under-graduate and post-graduate level, in particular in the field of materials science. He is main coordinator / partner in international and national projects. Prof. Pissis has published more than 230 journal papers, more than 80 papers in conference proceedings and 11 book chapters. He has more than 350 contributions to international conferences and more than 80 to national conferences.